Molecular Dynamics Simulation Study of Lanthanide Ions Ln^{3+} in Aqueous Solution Including Water Polarization. Change in Coordination Number from 9 to 8 along the Series

Th. Kowall, F. Foglia, L. Helm,* and A. E. Merbach*

Contribution from the Institut de Chimie Minérale et Analytique, Université de Lausanne, Bâtiment de chimie (BCH), CH-1015 Lausanne-Dorigny, Switzerland

Received November 11, 1994[⊗]

Abstract: Classical molecular dynamics simulations have been carried out for lanthanide ions Ln^{3+} in aqueous solution. For the Ln^{3+}−water interaction we propose a new three-body potential function that takes into account the mean polarization of water molecules in the first hydration shell and that has been fitted to ab-initio results. By a usual pair potential approach we can reproduce the experimental distance of the first maximum in the cation−oxygen radial pair distribution function, but the first hydration shell is by far too unstable from both a structural and a dynamical point of view. Inclusion of a polarization term leads to a perfect agreement with coordination numbers from neutron diffraction studies as well as to decreased kinetic lability of the first hydration shell that is more consistent with experimental evidence. Notably, a coordination number of 8.5 is obtained for the middle of the lanthanide series and corresponds to an equilibrium between a 9-coordinated and an 8-coordinated Ln^{3+}−aqua ion. Water exchange rate constants from computer simulations are reported for the first time for Ln^{3+}−aqua ions. A maximum of the exchange rate constants in the middle of the series is in agreement with the current interpretation of experimental data, based on the change of relative stability of the ennea and octa aqua ions along the series.

1. Introduction

This paper is the starting point in an effort to develop a microscopic picture of the water exchange on tripositive lanthanide ions (henceforth referred to as Ln^{3+}) in solution (eq 1) by means of classical molecular dynamics simulations (MD).

$$Ln(H_2O)_n^{3+} + {}^*H_2O \rightarrow [\ddagger] \rightarrow Ln(H_2O)_{n-1}{}^*H_2O^{3+} + H_2O \quad (1)$$

We propose an improved description of the Ln^{3+}−water interaction and check the quality of the simulations by comparison with fundamental structural and kinetic data from experimental measurements. In our future work we will focus on the nature of the transition state [‡] in eq 1 and on the microscopic mechanism of the water exchange reaction.

Across the series of Ln^{3+} ions the inner 4f orbitals are progressively filled. The ionic radius shrinks from 1.16 Å for La^{3+} to 0.98 Å for Lu^{3+} [1] due to the increasing nuclear charge. This allows one to study the effects of changing ion size on various chemical properties without interference from crystal field effects. In recent years the coordination of Ln^{3+} in various solvents has been extensively studied by a variety of experimental techniques (e.g., refs 2 and 3). The principal information gained concerns coordination numbers, the radial structure of the solvation shell, the hydration enthalpy, and the kinetic parameters of the solvent exchange. Experimental results for some Ln^{3+}−water systems are given in Table 1. In addition two computer simulation studies of Ln^{3+} in solution have been published. In a MD study Meier et al.[7] studied the concentration dependence of structural quantities of aqueous solutions of $LaCl_3$ using a flexible water model to account for the polarization of water. One result they found was a concentration-dependent coordination number for the La^{3+} ion, increasing from 10.2 at 2 *m* concentration to 12 at "infinite" dilution (1 La^{3+} ion and 200 water molecules). Galera et al.[8] reported a preliminary Monte Carlo simulation of Ln^{3+} ions in aqueous solution. Using effective pair potentials, they studied the change in the coordination number across the series and qualitatively the mechanism of water exchange.

The feasibility and usefulness of classical molecular dynamics simulations of the solvation of Ln^{3+} in solvents such as water or dimethylformamide are due to the nondirectional interaction without covalent contributions between the hard Ln^{3+} ion and oxygen-donor solvent molecules. Hence, for these solvents, the ion−solvent forces should be well represented by simple Coulomb and van der Waals terms. At the same time the change in the rate or the mechanism of the solvent exchange reaction along the series of Ln^{3+} ions should be mainly due to spatial packing effects and nonbonding interactions in the first solvation shell and not due to differences in the electronic structure of the cation.[9] From a methodological point of view this constitutes an ideal problem to be addressed by classical MD

[⊗] Abstract published in *Advance ACS Abstracts*, March 15, 1995.

(1) Shannon, R. *Acta Crystallogr.* **1976**, *A32*, 751.

(2) Rizkalla, E. M.; Choppin, G. In *Handbook on the Physics and Chemistry of Rare Earths*; Gschneider, K. A., Eyring, L., Eds.; Elsevier: North-Holland, 1991; Vol. 15.

(3) Lincoln, S. F.; Merbach, A. E. *Substitution Reactions of Solvated Metal Ions* In: *Advances in Inorganic Chemistry*; Academic Press: New York, 1995; Vol. 42, in press.

(4) Structural data are from neutron diffraction experiments: (a) Cossy, C.; Barnes, A. C.; Enderby, J. E.; Merbach, A. E. *J. Chem. Phys.* **1989**, *90*, 3254. (b) Helm, L.; Merbach, A. E. *Eur. J. Solid State Inorg. Chem.* **1991**, *28*, 245. (c) Cossy, C.; Helm, L.; Powell, D. H.; Merbach, A. E. *New J. Chem.* **1995**, *19*, 27.

(5) *Gmelin Handbuch der Anorganischen Chemie, Seltenerdelemente, Teil B7*; Springer: Berlin, 1976.

(6) Exchange rate constants from NMR experiments: (a) Cossy, C.; Helm, L.; Merbach, A. E. *Inorg. Chem.* **1989**, *28*, 2699. (b) Micskei, K.; Powell, D. H.; Helm, L.; Brücher, E.; Merbach, A. E. *Magn. Reson. Chem.* **1993**, *31*, 1011. (c) Powell, D. H.; Merbach, A. E. *Magn. Reson. Chem.* **1994**, *32*, 739.

(7) Meier, W.; Bopp, Ph.; Probst, M. M.; Spohr, E.; Lin, J. L. *J. Phys. Chem.* **1990**, *94*, 4672.

(8) Galera, S.; Lluch, J. M.; Oliva, A.; Bertrán, J.; Foglia, F.; Helm, L.; Merbach, A. E. *New J. Chem.* **1993**, *17*, 773.

(9) Hengrasmee, S.; Probst, M. M. *Z. Naturforsch.* **1991**, *46a*, 117.

0002-7863/95/1517-3790$09.00/0

Table 1. Experimental Structural, Thermodynamic, and Kinetic Data for Lanthanide(III) Ions in Aqueous Solution

	ref	Nd^{3+}	Sm^{3+}	Gd^{3+}	Dy^{3+}	Yb^{3+}
r_{LnO}/Å	4	2.50_8	2.46_7		2.38_6	2.32_8
FWHH[a]/Å	4	0.28	0.31		0.26	0.24
CN	4	8.9_9	8.5_4		7.9_9	7.9_4
ΔH_{sol}/(kcal mol^{-1})	5	−822.5	−839.0	−851.9	−867.1	−893.9
water exchange rate constant k_{ex}^{298} [b]/ns^{-1}	6	≥0.5		1.19	0.43	0.05
number of exchange events per time k/ns^{-1}		≥4.5		10	3.4	0.4

[a] FWHH is the full width at half-height of the first peak in the experimental distribution function. [b] k_{ex}^{298} is the exchange rate constant of a particular water molecule; $k = k_{ex}^{298} \cdot CN$.

simulations. Moreover, from a practical point of view, the residence time of a water molecule in the first hydration sphere lies in the subnanosecond regime (see Table 1) and therefore within the reach of MD simulations carried out on today's workstations.

What makes the simulation of aqueous solutions of Ln^{3+} considerably more demanding compared to simulations of, e.g., alkali metal ions[10] is the high positive charge density of the Ln^{3+} ion. It is questionable whether the polarization of water due to Ln^{3+} can be reasonably taken into account by an effective pair potential. To elucidate this point, we performed two simulation series: a first one based on an empirical effective pair potential and a second one with explicit inclusion of a polarization term. In the literature several groups have proposed approaches to improve the description of ionic solutions in computer simulations by including polarization effects (e.g., refs 11−15). The most well-known is the iterative approach of Kollman et al.[14] In this model, polarizable point dipoles are placed on the atomic sites and the electric field equations are solved in an iterative, rather time-consuming manner. Because water exchange events for Ln^{3+} are rare on the typical time scale of MD simulations, fairly long simulation runs (at least 1 ns) are necessary to obtain a sufficient statistical basis. Consequently, the time-consuming iterative methods are not applicable. However, as a more efficient way to take into account a polarization effect, we can take advantage of the strong radial orientation of the water dipole vectors around a cationic charge of +3 by simply scaling the water dipole moment as a function of the ion−water distance. This new approach will be presented here. After an outline of the simulations performed, we report then the results with the unpolarizable and the polarizable water models. Finally, we discuss the results in relation to available experimental data.

2. Method To Account for the Polarization of Water around Ln^{3+}

2.1. Scaling of the Electric Dipole Moment of a Water Molecule. The first-order approximation to treat the electrostatic interaction between a lanthanide ion Ln^{3+} and a water molecule is to describe it as the interaction between a static point charge of +3 and the point charges assumed on a water molecule according to the chosen water model (e.g., the model TIP3P[16] or SPC[17]). This is an extrapolative approach that assumes complete transferability of the values of the point charges that have not been parametrized on any experimental or quantum chemical data for the Ln^{3+}−water interaction. It is, however, by no means evident that the static point charges that have been found to describe the water−water interaction in pure water are also the best possible choice for the Ln^{3+}−water interaction. Static water charges optimized for simulations of pure liquid water are simply "effective" charges that yield the correct total energy of the system and to some extent take into account many-body effects in liquid water. Furthermore, given the considerable positive charge of a lanthanide ion, it is evident that the polarization of the water molecules due to the ion may substantially influence both the ion−water *and* the water−water interaction in the first hydration shell and should be included explicitly in the potential energy function, not just implicitly as an effective pair potential. It is too drastic an approximation to suppose that "effective" static water charges are directly able to describe the non-negligible many-body effects for the Ln^{3+}−water interaction.

For Monte Carlo simulations of divalent transition metal ions Rode et al.[18,19] improved a conventional pair potential function by adding an oxygen−oxygen repulsion term for water molecules in the neighborhood of the ion. In this way they took into account the most relevant three-body interaction effects, and in Monte Carlo simulations of a Cu^{2+} [18] as well as of a Zn^{2+} ion[19] in aqueous solution the coordination number was significantly lowered to values in agreement with experimental findings. Analytical derivatives for the proposed interaction model−necessary for MD simulations−were not given in refs 18 and 19.

In this paper we present an alternative and physically transparent route to incorporate a polarization effect. We propose to scale up the permanent electric dipole moment of water as a function of the ion−water distance by a factor of $1 + fS(r)$):

$$q_i = q_i^{\circ}(1 + fS(r_{\alpha,cm-ion})) \qquad (2)$$

$$i \in \{O,H1,H2\} \text{ of water molecule } \alpha$$

$$S(r \to \infty) = 0$$

$$\vec{r}_{\alpha,cm} = (1/M_{H_2O})(m_H\vec{r}_{H1} + m_H\vec{r}_{H2} + m_O\vec{r}_O)$$

$$r_{\alpha,cm-ion} = |\vec{r}_{\alpha,cm} - \vec{r}_{ion}|$$

The subscript i stands for each atom of a water molecule, and q_i° are the corresponding unscaled point charges. The distance between the ion and the center of mass of a water molecule α is denoted by $r_{\alpha,cm-ion}$. The scaling function $S(r)$ is chosen to be unity if r is less than a cutoff distance R_1. The parameter $1 + f$ is the maximum scaling of the water charges and is the essential potential parameter to be determined in section 2.3. By applying a common scaling factor to the whole water molecule α, its electric neutrality is not affected.

Kollman et al. have proposed a more rigorous way to handle the polarization, e.g., for alkali metal ions in aqueous solution.[14,15] In their approach, polarizable point dipoles are assumed at the sites of the atoms and the induced dipole moments are evaluated by solving the electric field equations

(10) Impey, R. W.; Madden, P. A.; McDonald, I. R. *J. Phys. Chem.* **1983**, *87*, 5071.
(11) Sprik, M.; Klein, M. L.; Watanabe, K. *J. Phys. Chem.* **1990**, *94*, 6483.
(12) Zhu, S.-B.; Robinson, G. W. *J. Chem. Phys.* **1992**, *97*, 4336.
(13) Lybrand, T. P.; Kollman, P. A. *J. Chem. Phys.* **1985**, *83*, 2923.
(14) Caldwell, J.; Dang, L. X.; Kollman, P. A. *J. Am. Chem. Soc.* **1990**, *112*, 9144.
(15) Dang, L. X.; Rice, J. E.; Caldwell, J.; Kollman, P. A. *J. Am. Chem. Soc.* **1991**, *113*, 2481.
(16) Jorgensen, W. L.; Chandrasekhar, J.; Madura, J. D.; Impey, R. W.; Klein, M. L. *J. Phys. Chem.* **1983**, *79*, 926.
(17) Berendsen, H. J. C.; Postma, J. P. M.; van Gunsteren, W. F.; Hermans, J. In *Intermolecular Forces*; Pullman, B., Ed.; Reidel: Dordrecht, The Netherlands, 1981.
(18) Rode, B. M.; Islam, S. M. *Z. Naturforsch.* **1991**, *46a*, 357.
(19) Yongyai, Y. P.; Kokpol, S.; Rode, B. M. *Chem. Phys.* **1991**, *156*, 403.
(20) Kepert, D. L. *Inorganic Stereochemistry* (Inorganic chemistry concepts 6); Springer: Berlin, Heidelberg, New York, 1982; Chapter 12.

in an iterative manner. Due to the iterative procedure employed, computational costs increase by a factor of 2−10 compared to simulations without polarizable point dipoles.[14] Our proposition lies between the unpolarizable models and the iterative "many-body potentials" and is of less general applicability. However, as an advantage, computational costs increase only by about 10% compared to simulations with static point charges for water, so that longer simulation runs are possible. We take advantage of a particular feature of the systems studied here, namely, the strong radial alignment of the water dipole in the first hydration shell around a positive charge of +3 (refer to section 5). This allows us to take account of polarization by simply enlarging the value of the permanent dipole moment of a water molecule without changing its direction within the molecular coordinate system. In a more general view, this is an example of how, in computational chemistry, a more general and more sophisticated approach can be boiled down to a more efficient and more transparent one for a particular system.

In the following it remains to decide on an analytical form for $S(r)$, to present the analytical expressions for the resulting forces with the new potential function, to determine the parameter f, and to readjust the parameters for the Ln^{3+}−water Lennard-Jones interaction.

2.2. Analytical Form of the Scaling Function $S(r)$. Given the overall degree of simplification concerning the description of the molecular interactions in a molecular mechanics approach, the actual analytical form for $S(r)$ should not be too critical. We used an analytical form that is already used in MD work as a switching function for the electrostatic interaction at the cutoff radius.[21] In our case it allows a smooth transition from zero to maximum polarization in a well-defined distance range between R_1 and R_2.

$$S(r) = \begin{cases} 1 & \text{for} \quad r < R_1 \\ \dfrac{(R_2 - r)^2(R_2 + 2r - 3R_1)}{(R_2 - R_1)^3} & \text{for } R_1 < r < R_2 \\ 0 & \text{for} \quad r > R_2 \end{cases} \tag{3}$$

$$\frac{\partial S(r)}{\partial r} = \begin{cases} 0 & \text{for} \quad r < R_1 \\ 6\dfrac{(R_2 - r)(R_1 - r)}{(R_2 - R_1)^3} & \text{for } R_1 < r < R_2 \\ 0 & \text{for} \quad r > R_2 \end{cases} \tag{4}$$

We have chosen a distance range with $R_1 = 2.1$ Å and $R_2 = 4.0$ Å. In this way the scaling procedure only affects the first hydration shell of a lanthanide ion and does not need to be considered for water molecules beyond this shell.[4] The actual functional behavior below $R_1 = 2.1$ Å is of no relevance, since such small distances are very improbable for the systems Ln^{3+}/H_2O.

2.3. Analytical Expressions for the Electrostatic Forces. For practical reasons the ion−water and the water−water interactions have to be treated separately. Because a common scaling factor $(1 + fS(r))$ applies to the whole water molecule and depends on its center of mass, the interactions between single point charges can no longer be treated individually. Instead, the derivative of the *total* electrostatic energy between the ion and a water molecule α or between two water molecules α and β has to be evaluated.

Electrostatic Interaction between the Cation and a Water Molecule α. The electrostatic forces for the ion−water interaction consist of the ordinary Coulomb force, multiplied by the scaling factor, plus an additional term resulting from the distance dependence of the scaling factor itself:

$$V^C_{\alpha,\text{ion}}(r_{\alpha,i-\text{ion}}, r_{\alpha,\text{cm}-\text{ion}}) = (1 + fS(r_{\alpha,\text{cm}-\text{ion}}))\sum_{i=1}^{3}\frac{1}{4\pi\epsilon_0}\frac{q_{\text{ion}}q_i^\circ}{r_{\alpha,i-\text{ion}}} \tag{5a}$$

$i \in \{O,H1,H2\}$ of water molecule α

$$\vec{F}^C_{\alpha,i} = -\frac{\partial V^C}{\partial \vec{r}_{\alpha,i}}$$

$$= +(1 + fS(r_{\alpha,\text{cm}-\text{ion}}))\frac{1}{4\pi\epsilon_0}\frac{q_{\text{ion}}q_i^\circ}{r^2_{\alpha,i-\text{ion}}}\frac{\vec{r}_{\alpha,i-\text{ion}}}{r_{\alpha,i-\text{ion}}} - \left(\sum_{k=1}^{3}\frac{1}{4\pi\epsilon_0}\frac{q_{\text{ion}}q_k^\circ}{r_{\alpha,k-\text{ion}}}\right) f\frac{\partial S(r_{\alpha,\text{cm}-\text{ion}})}{\partial r_{\alpha,\text{cm}-\text{ion}}}\frac{\partial r_{\alpha,\text{cm}-\text{ion}}}{\partial \vec{r}_{\alpha,i}} \tag{5b}$$

$$\frac{\partial r_{\alpha,\text{cm}-\text{ion}}}{\partial \vec{r}_{\alpha,i}} = \frac{m_i}{M_{H_2O}}\frac{\vec{r}_{\alpha,\text{cm}-\text{ion}}}{r_{\alpha,\text{cm}-\text{ion}}} \tag{5c}$$

$$\vec{F}^C_{\text{ion}} = -\sum_{i=1}^{3}\vec{F}^C_{\alpha,i} \tag{5d}$$

The subscript i stands for each atom of the water molecule α. The q_i° are the unscaled point charges of atom i of a water molecule, and $r_{\alpha,i-\text{ion}}$ represents the distance between the atom i of water molecule α and the ion. $V^C_{\alpha,\text{ion}}$ is the electrostatic energy between water molecule α and an Ln^{3+} ion ($q_{\text{ion}} = +3$). $\vec{F}^C_{\alpha,i}$ and $\vec{F}^C_{\text{ion}}$ denote the electrostatic force on atom i of water molecule α and the force on the ion, respectively.

Electrostatic Interaction between a Water Molecule α and a Water Molecule β. The same procedure applies to the water−water interaction. In our model the water charges and therefore the water−water electrostatic energy depend on the ion position. Consequently, the derivative of the Coulomb energy with respect to the ion position no longer equals zero as in a model with static point charges. As a result, besides the water−water forces in direction $\vec{r}_{\alpha,i-\beta,j}$, there are additional water−ion forces in the directions $\vec{r}_{\alpha,\text{cm}-\text{ion}}$ and $\vec{r}_{\beta,\text{cm}-\text{ion}}$. This illustrates the fact that, when polarization is included, interactions are no longer simply pairwise additive and all water−ion−water trimers, where at least one water molecule belongs to the first hydration shell of the ion, must be described by a three-body interaction.

$$V^C_{\alpha,\beta}(r_{\alpha,i-\beta,j}, r_{\alpha,\text{cm}-\text{ion}}, r_{\beta,\text{cm}-\text{ion}}) = (1 + fS(r_{\alpha,\text{cm}-\text{ion}}))(1 + fS(r_{\beta,\text{cm}-\text{ion}}))\sum_{ij}\frac{1}{4\pi\epsilon_0}\frac{q_i^\circ q_j^\circ}{r_{\alpha,i-\beta,j}} \tag{6a}$$

$i \in \{O,H1,H2\}$ of water molecule α

$j \in \{O,H1,H2\}$ of water molecule β

(21) van Gunsteren, W. F.; Berendsen, H. J. C.; BIOMOS b.v., Biomolecular Software; Laboratory of Physical Chemistry, University of Groningen.

$$\vec{F}^{C}_{\alpha,i} = -\frac{\partial V^{C}}{\partial \vec{r}_{\alpha,i}}$$

$$= +(1 + fS(r_{\alpha,\mathrm{cm-ion}}))(1 + fS(r_{\beta,\mathrm{cm-ion}})) \times \sum_{j=1}^{3} \frac{1}{4\pi\epsilon_0} \frac{q_i^o q_j^o}{r^2_{\alpha,i-\beta,j}} \frac{\vec{r}_{\alpha,i-\beta,j}}{r_{\alpha,i-\beta,j}} - (1 + fS(r_{\beta,\mathrm{cm-ion}})) \times \left(\sum_{ij} \frac{1}{4\pi\epsilon_0} \frac{q_i^o q_j^o}{r_{\alpha,i-\beta,j}}\right) f \frac{\partial S(r_{\alpha,\mathrm{cm-ion}})}{\partial r_{\alpha,\mathrm{cm-ion}}} \frac{\partial r_{\alpha,\mathrm{cm-ion}}}{\partial \vec{r}_{\alpha,i}} \quad (6b)$$

$$\frac{\partial r_{\alpha,\mathrm{cm-ion}}}{\partial \vec{r}_{\alpha,i}} = \frac{m_i}{M_{H_2O}} \frac{\vec{r}_{\alpha,\mathrm{cm-ion}}}{r_{\alpha,\mathrm{cm-ion}}} \quad (6c)$$

For $\vec{F}^{C}_{\beta,j}$ an expression analoguous to $\vec{F}^{C}_{\alpha,j}$ applies.

$$\vec{F}^{C}_{\mathrm{ion}} = -\sum_{i=1}^{3} \vec{F}^{C}_{\alpha,i} - \sum_{j=1}^{3} \vec{F}^{C}_{\beta,j} \neq 0 \quad (6d)$$

The symbols have the same meaning as in the preceding paragraph. $V^{C}_{\alpha,\beta}$ is the electrostatic energy between water molecule α and water molecule β. The distance between atom i of water molecule α and atom j of water molecule β is denoted as $r_{\alpha,i-\beta,j}$.

2.4. Parametrization of the Ion–Water Interaction. By introducing a maximum charge upscaling factor $(1 + f)$, the parameter space for the potential function has increased by one dimension. In the following, the parametrization strategy pursued for the ion–water interaction will be presented.

The parameter f has been fixed with reference to ab-initio calculations at the Hartree–Fock level of Hengrasmee and Probst[9] on $Ln(H_2O)_8^{3+}$ clusters. In ref 9 the potential energy as a function of the Ln^{3+}–water distance has been calculated for a coordination number (CN) of 8 along the whole series of lanthanide ions from La^{3+} to Lu^{3+} in a distance range from 2.1 to 3.1 Å. However, an inconvenience from our perspective is that, in ref 9, calculations are based on a cubic instead of a square antiprismatic arrangement of the eight water molecules. A cubic arrangement is intrinsically less stable than an antiprismatic one[20] and therefore less probable in MD simulations, but its higher symmetry reduces computational costs in quantum chemical calculations. In addition, in ref 9, the energy minimum for the interaction between Ln^{3+} and *one* water molecule is given both at the Hartree–Fock level and with inclusion of the correlation energy by means of Moeller–Plesset second-order perturbation theory (MP2).

In Figure 1 the results from ref 9 for Nd^{3+} and Yb^{3+} are compared to our approach when eight TIP3P molecules are placed on a sphere and the value for f is increased from 0.0 to 0.4. Because the orientation of the HH vectors was neither given explicitly in ref 9 nor fixed by the cubic symmetry for the water oxygens, we generated clusters $Ln(H_2O)_8^{3+}$ with radially aligned water dipole vectors and subsequently minimized the potential energy with respect to the HH orientation. At this stage the parameters for the ion–oxygen Lennard-Jones interaction are those from the unpolarizable model (Table 2) that yield a radius of the first hydration shell in agreement with experimental structural results.

Undoubtedly, the depth of the potential well is too shallow in the unpolarizable model and charge upscaling leads to a clear improvement in reproduction of the ab-initio result for both Nd^{3+} and Yb^{3+}, in particular for the energy minimum of $Ln(H_2O)_1^{3+}$. For Nd^{3+} and Yb^{3+} values of $f = 0.3$ and $f = 0.35$, respectively,

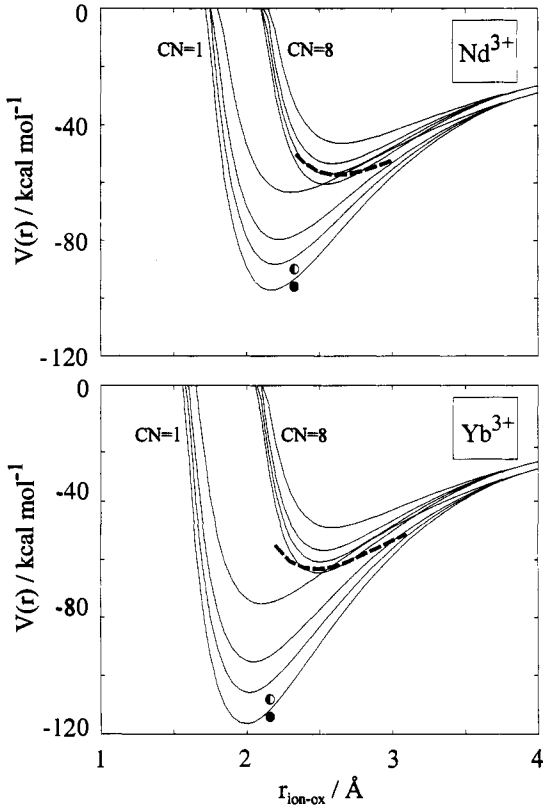

Figure 1. Potential energy of a cluster $Ln(H_2O)_8^{3+}$ with cubic symmetry (CN = 8) and of $Ln(H_2O)_1^{3+}$ (CN = 1) as a function of the ion–oxygen distance for values of the fitting parameter $f = 0.0$, 0.2, 0.3, and 0.4 (solid lines, top to bottom) for neodymium and ytterbium. Ab-initio results from ref 9 are included for comparison (dashed line for CN = 8, half-filled circle for CN = 1 at the Hartree–Fock level, and filled circle for CN = 1 at the MP2 level).

Table 2. Parameters for the 8–6 Lennard-Jones Interaction between Ln^{3+} and a Water Oxygen

	A_{io}/(kcal mol^{-1} Å^8)	B_{io}/(kcal mol^{-1} Å^6)		A_{io}/(kcal mol^{-1} Å^8)	B_{io}/(kcal mol^{-1} Å^6)
Nd_{up}	16 250	190	Nd	21 000	190
Sm_{up}	11 580	170	Sm	16 000	170
Yb_{up}	8 600	0	Yb	8 600	0

give the best adjustment to the depth of the potential minimum. However, since the ab-initio calculations for CN = 8 were only possible at the Hartree–Fock level and are therefore of limited accuracy (cf. the ab-initio energy for CN = 1 with and without inclusion of the correlation energy in Figure 1), we did not try to fit the ion dependence of the polarization term, but considered it more consistent to fit all potential energy curves with the same f. We fixed the maximum charge upscaling factor to $1 + f = 1.3$. An increase of 30% of the water dipole moment due to the proximity of a Ln^{3+} ion is quite reasonable when compared to the increase of 24% that has been calculated with the more rigorous and time-consuming approach of ref 14 for the transfer of a water molecule from the gas phase to liquid water.

Finally, it remains to readjust the Lennard-Jones parameters for the ion–oxygen interaction in the polarizable model. For the Lennard-Jones part of the ion–oxygen interaction we have throughout lowered the repulsive exponent from the general used value of 12 to 8. Whereas a r^{-6} law for the Lennard-Jones attraction is physically justifiable as the interaction between induced electric dipoles, the power law r^{-m} with $m = 12$ is commonly used only for reasons of computational efficiency. Indeed, an exponential law for the repulsion between nuclei can be expected from quantum mechanical considerations. A

Table 3. Overview of Simulation Parameters

	pure water	Nd_{up}	Sm_{up}	Yb_{up}	Nd	Sm	Yb
number of Ln^{3+} ions	0		1			1	
number of TIP3P molecules	300		300			300	
time step Δt/fs	1.0		1.0			1.0	
simulation time/ps	65		262			1048	
stored configurations	1024		8192			32768	
cutoff r_{co}/Å	8.5		8.5			8.5	
τ_T/ps	0.1		0.1			0.1	
τ_p/ps	0.5		0.5			0.5	
density/(g/cm^3)	1.029	1.032	1.038	1.038	1.006	1.013	1.023
temperature/K	301.1	302.4	302.7	302.5	301.8	301.9	302.0
$E_{water-water}$/kcal	−2910	−2467	−2450	−2442	−2412	−2407	−2383
$E_{ion-water}$/kcal		−1065	−1115	−1143	−1202	−1246	−1348

smoother Lennard-Jones repulsion of the form

$$V^{LJ}_{ion-ox}(r_{ion-ox}) = \frac{A_{io}}{r^{m}_{ion-ox}} - \frac{B_{io}}{r^{6}_{ion-ox}} \qquad m = 8 \qquad (7)$$

results in a broadening of the first maximum of the pair distribution $g_{ion-oxygen}(r)$ and improves the agreement with the radial distribution function obtained from neutron diffraction.

Unfortunately, the potential energy curves from ref 9 are dominated by the water−water repulsion part and are rather insensitive to the actual choice of the Lennard-Jones parameters for the ion−water interaction. In fact, a change in A_{io}/B_{io} parameters for the ion−oxygen interaction that clearly influences the coordination of the ion is hardly perceptible in the potential energy curves. Therefore, in pretrial runs, A_{io}/B_{io} parameters were optimized to yield the most stable solvation shell of eight or nine water molecules, respectively. As a guideline, a solvation shell is taken to be more stable the more distinct the plateau region between the first and second hydration spheres in a plot of the running coordination number $CN_{ion-oxygen}(r)$ of the ion. This choice of parameters can be justified by the fact that our MD simulations always tend to yield faster water exchange than that observed experimentally and that even a slight increase in the coordination number between the first and second hydration sphere, indicative of a water molecule staying temporarily between these spheres, increases the water exchange rates further.

The two parameter sets for integer hydration numbers of 8 and 9 were supplemented by a third one for a hydration number of 8.5.

3. Simulation Outline

All molecular dynamics runs were performed using the program package GROMOS86[21]—modified to incorporate the potential function from section 2—on a Silicon Graphics Indigo 2 workstation. For the unscaled water point charges q_i^o, the oxygen−oxygen van der Waals interaction, and the water geometry, we used the rigid TIP3P model from Jorgensen et al.[16] We abstained from using a flexible water model, which would demand a considerably shorter integration step, but would not substantially improve long−time equilibrium properties of liquid water.[22]

We carried out two simulation series, the first with static "unpolarizable (up)" point charges ($f = 0.0$) and the second with inclusion of water polarization ($f = 0.3$) as described in section 2. In each series we intended to stick to three ion−oxygen Lennard−Jones parameter sets that result in coordination numbers of 8, 8.5, and 9 and are taken as representative model systems for Nd^{3+}, Sm^{3+}, and Yb^{3+} (cf. ref 4b). For the first simulation series with unpolarizable water molecules (Nd_{up}, Sm_{up}, Yb_{up}), parameters were empirically fixed to reproduce the experimental distance of the first maximum in $g_{ion-oxygen}(r)$ as well as the desired coordination number. For the second simulation series (Nd, Sm, Yb) the parametrization strategy described in section 2 was adopted.

(22) Guàrdia, E.; Padró, J. A. *J. Phys. Chem.* **1990**, *94*, 6049.

Table 4. Structural and Thermodynamic Results from the Simulations

	Nd_{up}	Sm_{up}	Yb_{up}	Nd	Sm	Yb
r_{LnO}/Å	2.43	2.33	2.28	2.43	2.33	2.21
FWHH/Å	0.22	0.22	0.23	0.18	0.17	0.18
ΔH_{sol}/(kcal mol^{-1})	−795	−830	−849	−877	−917	−994

These two simulation series were supplemented by a simulation of pure water, necessary for the calculation of the hydration enthalpy ΔH_{sol} of the Ln^{3+} cation.

Table 2 gives the parameters for the ion−oxygen Lennard-Jones interaction, whereas Table 3 summarizes the most important parameters of the NTP simulation runs, which were preceeded by equilibration periods of at least 60 ps. τ_T and τ_p are the relaxation times effective in the algorithm of Berendsen et al.[23] to keep the system at ambient temperature and pressure. The geometry of the water molecules is fixed by the procedure SHAKE.[24]

4. Results for Unpolarizable Water

In this section results for the unpolarizable model ($f = 0.0$) are given. These served mainly as a motivation to further improve the potential energy function by introducing a polarization term.

4.1. Structural and Thermodynamic Results. Figures 2 and 3 display the cation−water radial pair distribution function (dotted lines) and the running coordination number of the cation for the three simulations Nd_{up}, Sm_{up}, and Yb_{up}. For simulation Nd_{up} a coordination number of 9 is reasonably well defined. For simulation Sm_{up}, taken as a model for a coordination number of 8.5, a ninth water molecule is weakly associated with the inner shell of eight water molecules. For Yb_{up} no parameter set A_{io}/B_{io} could be found that resulted in a clear coordination number of 8. The curve shown is the best approximation when setting the parameter B_{io} for the Lennard-Jones ion−oxygen attraction to zero.

Table 4 gives the distance r_{LnO} and the full width at half-height (FWHH) of the first maximum in the radial pair distribution function $g_{ion-oxygen}(r)$ as well as the hydration enthalpy ΔH_{sol} of the ion. ΔH_{sol} was calculated from the water−ion interaction energy and the water−water reorganization energy (see Table 3) by applying the Born correction for a cutoff radius of 8.5 Å as in ref 8.

In ref 8 it was observed that, compared to the neutron diffraction result, the simulated peaks in $g_{ion-oxygen}(r)$ come out too narrow when a r^{-12} Lennard-Jones repulsion is used for the ion−oxygen interaction. We tried to resolve this problem by lowering the repulsive exponent m (see section 2.4), which leads indeed to a broadening of the first maximum in $g_{ion-oxygen}(r)$. Nevertheless, for $m = 8$, a value used throughout in our

(23) Berendsen, H. J. C.; Postma, J. P. M.; van Gunsteren, W. F.; DiNola, A.; Haak, J. R. *J. Chem. Phys.* **1984**, *81*, 3684.

(24) Ryckaert, J. P.; Ciccotti, G.; Berendsen, H. J. C. *J. Comput. Phys.* **1977**, *23*, 327.

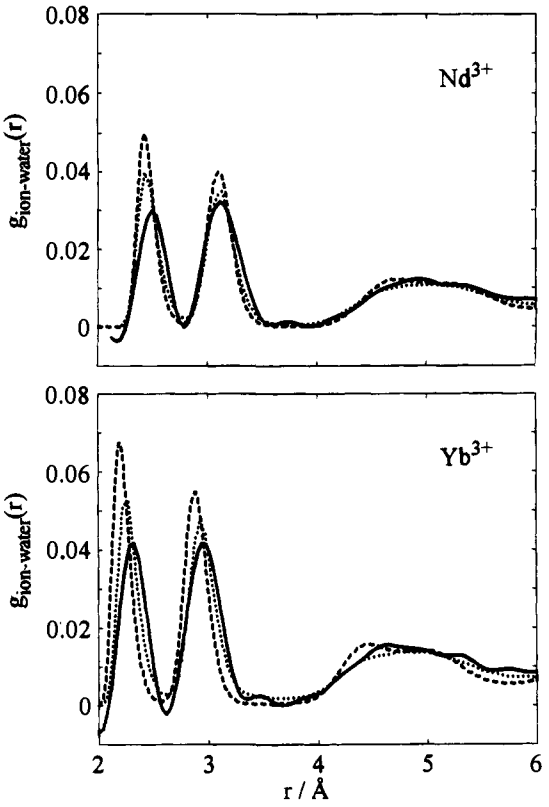

Figure 2. Comparison of the Ln^{3+}—water radial pair distribution function from the simulations (···, unpolarizable model; - - -, polarizable model) with experimental data from neutron diffraction (—, ref 4) for Nd^{3+} and Yb^{3+}. $g_{ion-water}(r)$ from the simulations are obtained by linear combination of $g_{ion-oxygen}(r)$ and $g_{ion-hydrogen}(r)$ using weighting factors from neutron scattering.

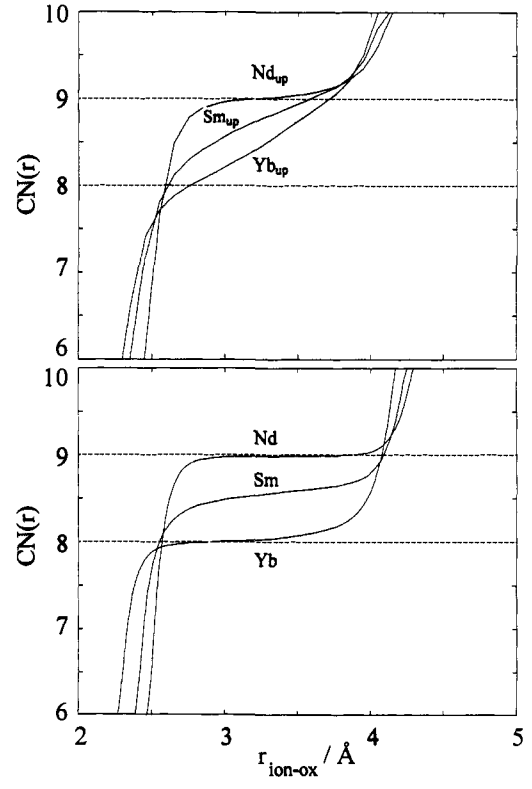

Figure 3. Running coordination number of Ln^{3+} for the simulations Nd_{up}, Sm_{up}, and Yb_{up} within the unpolarizable model ($f = 0.0$) and for the simulations Nd, Sm, and Yb within the polarizable model ($f = 0.3$).

simulations, the FWHH remains too small compared to the results from neutron diffraction studies (see Table 1 and Figure 2). The absolute value of the hydration enthalpy ΔH_{sol} and therefore the thermodynamic stability of a hydrated Ln^{3+} ion increase when going from a CN of 9 to CN 8, a result of the decreasing ionic radius. When compared to the experimental values (Table 1), hydration enthalpies ΔH_{sol} obtained from the simulations are slightly too positive. This indicates that, for the unpolarizable potential function, either the ion—water interaction is too weak or the water—water repulsion within the first hydration sphere is too strong.

4.2. Water Exchange. In the left-hand column of Figure 4 is shown the distance $r_{ion-ox}(t)$ for a 50-ps interval for all water molecules that at least once belong to the first hydration shell during the simulation time of 262 ps. In the right-hand column of Figure 4 the trajectories have subsequently been convoluted with a Gaussian function ($\sigma = 0.4$ ps) to suppress stochastic detail and to unveil the underlying characteristic features, i.e., exchange events and events where a water molecule enters the region between the first and second sphere but does not exchange. In Table 5 the extracted exchange rate constants are listed.

For simulation Nd_{up}, three exchange events and an "attempted" exchange event are clearly visible. For simulation Sm_{up}, a ninth water molecule loosely attached to the first hydration shell is perceptible in Figure 4. There are now so many exchange events that the time between two events nearly equals the duration of the exchange event itself. In simulation Yb_{up} the ninth water molecule has moved away from the first hydration shell and now stays preferably in the middle between the first and second hydration shells. Compared to the experimental solvent exchange rate constants (see Table 1), the simulated exchange is at least 2 orders of magnitude too fast.

In conclusion, from both a structural and a dynamical point of view, the first hydration shell appears to be too unstable within the unpolarizable model. Especially a coordination number of 8 is not realizable. In fact, the structural and dynamical deficiencies are interlinked: if the running coordination number $CN_{ion-oxygen}(r)$ does not exhibit a well-defined plateau region and therefore no well-defined coordination number (as is the case in Sm_{up} and Yb_{up}), a water molecule shuttling between the first and second hydration shells effectively lowers the residence time of a water molecule within the first hydration shell.

5. Results for Polarizable Water

The improvements obtained by applying the polarizable model ($f = 0.3$) are that a coordination number of 8 is now realizable and that solvent exchange rates are slowed by a factor of up to 12 toward the experimental values.

5.1. Structural and Thermodynamic Results. Figure 3 displays the running coordination number of the ion $CN_{ion-oxygen}(r)$ for the three simulations Nd, Sm, and Yb. Because $CN_{ion-oxygen}(r)$ exhibits a plateau region even for simulation Sm, structural hydration numbers CN are defined in all three cases: values of 9.0, 8.5, and 8.0 are obtained for simulations Nd, Sm, and Yb, respectively.

Figure 5 shows the distribution of the number of water molecules for three distance regions, i.e., the first and the second hydration shells as well as the region between the two shells. Before these numbers weer calculated, the trajectories $r_{ion-oxygen}(t)$ were convoluted with a Gaussian function ($\sigma = 0.4$ ps). In this way events where a water molecule from the first or second shell enters the region between the two shells only for a short time are suppressed and the coordination numbers obtained are more "effective" coordination numbers. The result reveals that the observed CN of 8.5 for simulation Sm corresponds indeed

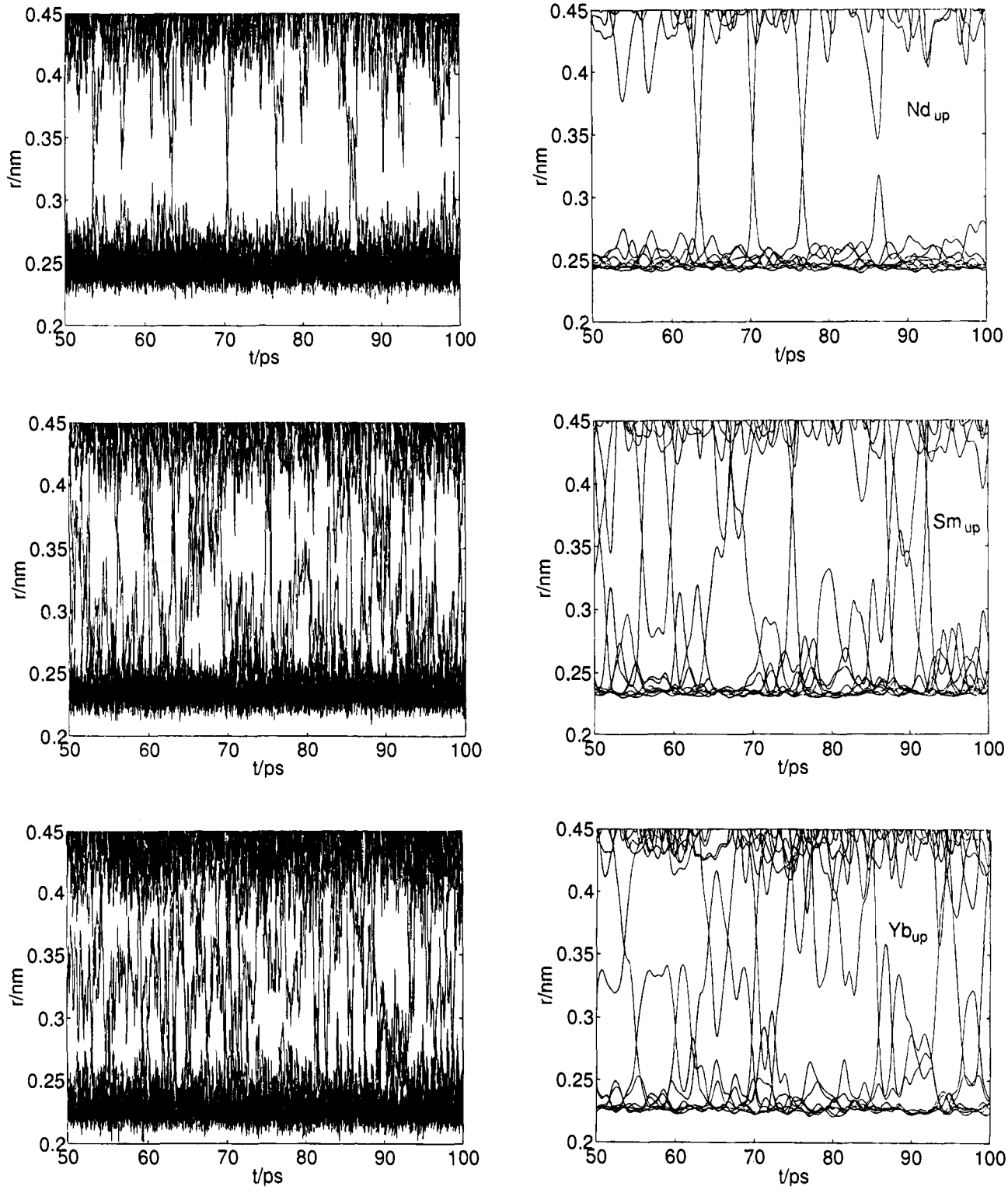

Figure 4. Ion−oxygen distance $r_{ion-ox}(t)$ for a 50-ps interval for the unpolarizable model ($f = 0.0$). The left column shows the unprocessed trajectories for simulations Nd_{up}, Sm_{up}, and Yb_{up} (from top to bottom). The right column displays the result after convolution with a Gauss function ($\sigma = 0.4$ ps).

Table 5. Water Exchange Rates from the Simulations

	Nd_{up}	Sm_{up}	Yb_{up}	Nd	Sm	Yb
number of exchange events observed in 1 ns	34	122	107	3	48	18
mean residence time τ_{res}/ns of a particular water molecule within the first shell	0.18	0.04	0.08	2.36	0.17	0.41
$k_{ex}^{298}/ns^{-1} = 1/\tau_{res}$	5.56	25	12.5	0.42	5.88	2.44

to an equilibrium between an octa aqua and an ennea aqua ion and, e.g., not to an 8-fold coordination with a ninth water molecule staying between the two shells. In only 9% of all configurations is a ninth water molecule present between the two spheres. The corresponding value for the unpolarizable model is 23%.

Inclusion of a polarization term in the potential function has a counteracting influence on the water−water and ion−water

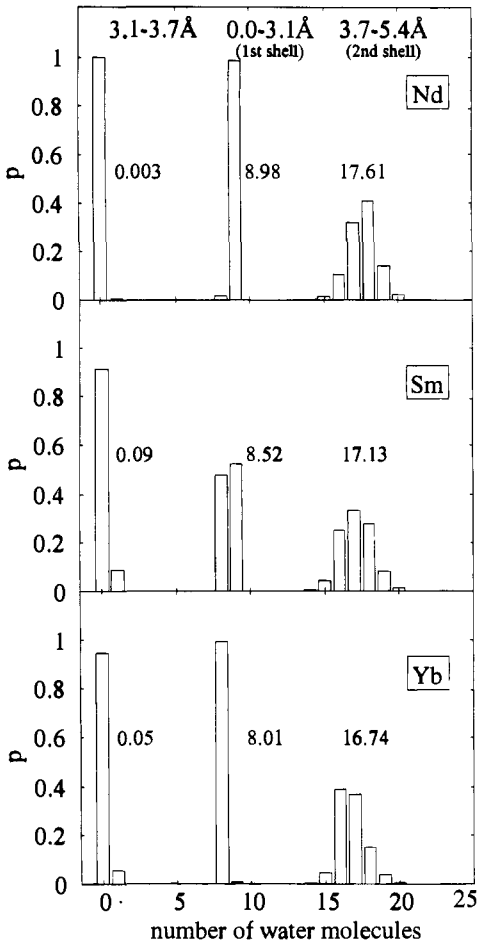

Figure 5. Distribution of the number of water molecules in three distance regions for the simulations Nd, Sm, and Yb within the polarizable model ($f = 0.3$). The inserted numbers are the mean number of water molecules in each distance range.

interaction energies (Table 3). A diminution of $E_{water-water}$ is overcompensated by an increased ion–water interaction $E_{ion-water}$. This results in more negative hydration enthalpies ΔH_{sol} compared to the unpolarizable model (Table 4). Yet, compared to experimental results (Table 1), the calculated ΔH_{sol} are now too negative, in particular for simulation Yb. This deficiency can at least partially be accounted for by the fact that the radius of the first hydration sphere r_{MO} for simulation Yb comes out to be too small by about 0.1 Å, when compared to the diffraction results for Yb^{3+}. The first hydration sphere is now more strongly bound to the ion with reduced radial mobility; i.e., the FWHH of the first maximum in $g_{ion-oxygen}(r)$ has shrunk further away from the diffraction result. This shortcoming is in line with the fact that the shape of the fitted potential curves in Figure 1 is narrower than the ab-initio result.

To prove the strong radial alignment of the water dipole vectors in the first hydration shell—a characteristic feature on which our polarization model is based—the corresponding angle distributions are depicted in Figure 6. The degree of alignment is only slightly further increased in the polarizable model. The mean tilt angles $\langle\theta\rangle$ of the water dipole vector from the cation–oxygen axis, calculated from simulations Nd, Sm, and Yb, are 13°, 13°, and 12° ± 7°, respectively.

Figure 7 shows the distribution of the angle $\angle(O_1 - H\cdots O_2)$ of a hydrogen bond between the first and second hydration shells and reveals a maximum at 180°. Together with the fact that the number of water molecules in the second hydration shell is approximately twice as great as that in the first shell (Figure 5) and that the dipole moment of water molecules in the second

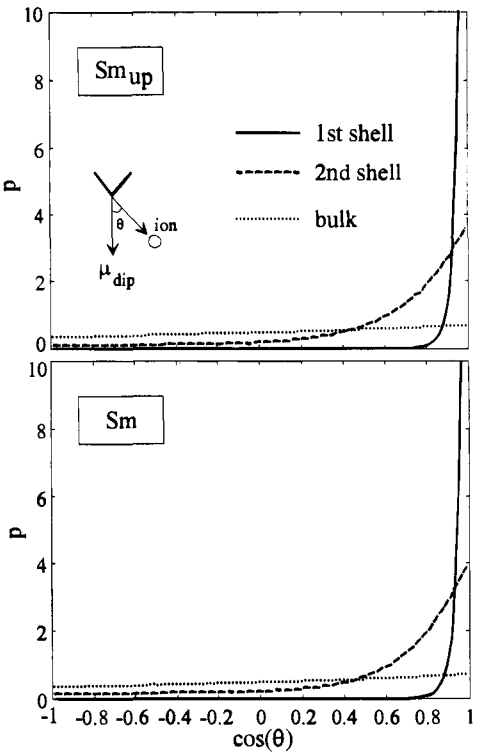

Figure 6. Distribution $p(\theta)$ of the angle θ between the dipole vector of a water molecule and the ion–oxygen distance vector.

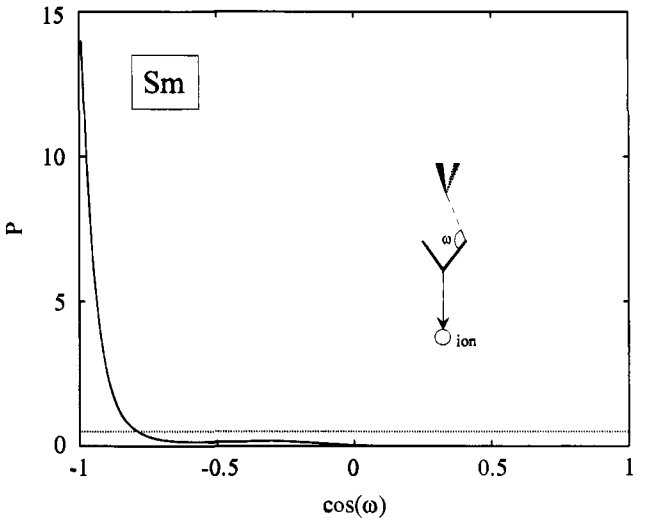

Figure 7. Distribution for the angle $\angle(O_1{-}H\cdots O_2)$ of hydrogen bonds between the first and second hydration shells. A geometric criterion has been applied to assign a hydrogen bond. For each water molecule in the second sphere (3.7 Å < r_{ion-ox} < 5.4 Å) the closest hydrogen atom of a water molecule in the first sphere (r_{ion-ox} < 3.1 Å) has been assigned.

shell is likewise preferentially radially aligned (Figure 6), a picture emerges where each water molecule of the first shell binds two water molecules by a linear hydrogen bond. It has to be conceded, however, that for real solutions results concerning the second hydration sphere might be already affected by inclusion of counterions and the existence of solvent-separated cation–anion pairs.

5.2. Water Exchange. In Figure 8 is shown the distance $r_{ion-oxygen}(t)$ for a 1000-ps interval after convolution with a Gaussian function ($\sigma = 0.4$ ps) and for all water molecules that belong to the first hydration shell at least once during the simulation time of 1048 ps. For simulation Sm the change between 8- and 9-fold coordination is much faster than for the two other lanthanides.

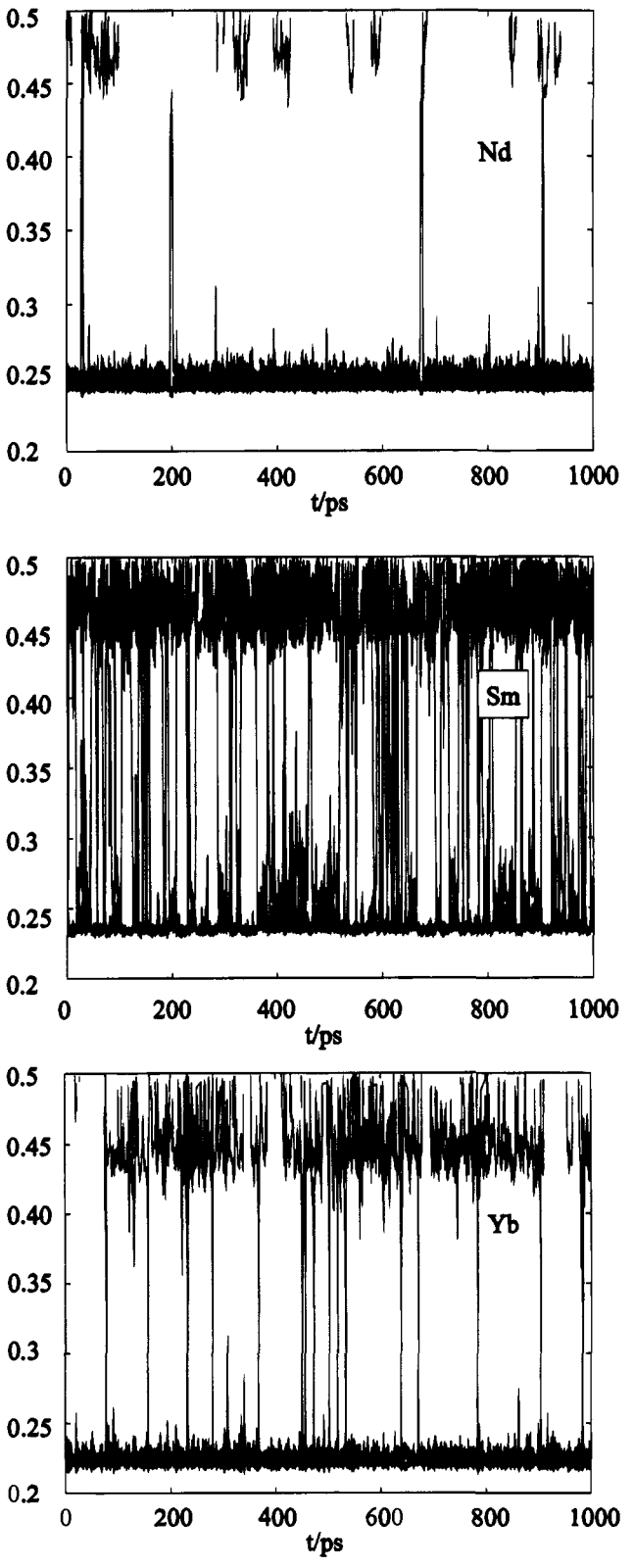

Figure 8. Ion–oxygen distance $r_{ion-ox}(t)$ for a 1000-ps interval for simulations Nd, Sm, and Yb (f = 0.3) after convolution of the trajectories with a Gauss function (σ = 0.4 ps). As in Figure 4 for reasons of clarity only trajectories of water molecules have been included that approach the ion by less than 3.8 Å at least one time. This accounts for the gaps in the second hydration shell.

In Figure 9 is plotted the probability $p(t)$ that a water molecule of the first hydration shell has never left the first hydration shell after a time t. The correlation function $p(t)$ is defined as in ref 10. A geometric definition of the first hydration shell that requires $r_{ion-oxygen} < 3.1$ Å was applied. The time constant from an exponential fit to $p(t)$ gives the mean residence time

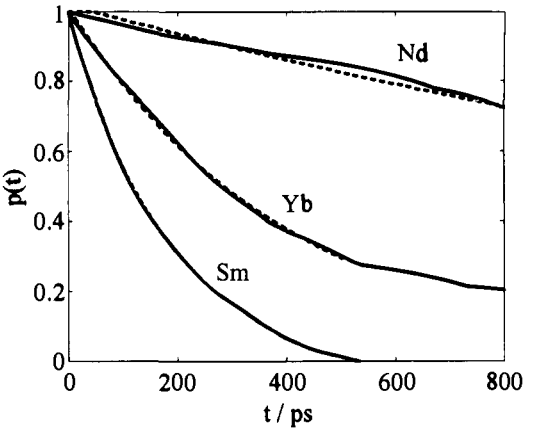

Figure 9. Residence probability $p(t)$ that a water molecule still belongs to the first hydration shell after a correlation time t calculated for the simulations Nd, Sm, and Yb (solid lines). Exponential fits are shown as dashed lines.

τ_{res} of a selected water molecule in the first hydration shell and is given in Table 5. The mean residence time τ_{res} of a selected water molecule divided by the coordination number is in agreement with the directly calculated value for the mean time between solvent exchange events.

Compared to the unpolarizable model the order of kinetic stability of the first hydration shell as a function of the coordination number CN has not changed, but the absolute exchange rates have been slowed by factors of 12, 6, and 2.5 for CN = 9, 8.5, and 8, respectively.

Given the long residence time of a water molecule in the first hydration sphere, in particular for simulation Nd, one might expect equilibration problems for the MD simulation. It is worth pointing out that in a series of test simulations of 16 ps, when the repulsive parameter A_{io} for the ion–oxygen Lennard-Jones interaction is changed and optimized, the coordination number of the ion always varied systematically. The system spontaneously becomes unstable when the interaction potential is changed and drops into the new stable state. Probably the presence of water molecules between the first and second shells for intermediate coordination numbers accelerates the equilibration process.

6. Discussion and Conclusions

A pair potential approach using static point charges for water does not yield a description of aqueous solutions of lanthanide ions Ln^{3+} in reasonable agreement with experimental results. In essence hydration shells turn out to be poorly defined structurally and too labile kinetically. In a broader frame we can point out again that restricting oneself to the reproduction of some experimental structural features such as the radius of the first hydration shell while neglecting the dynamical behavior may be a rather insensitive and insufficient criterion to judge the quality of a simulation.

As a scheme to incorporate a polarization effect in a less time-consuming manner than the usual iterative methods, we have proposed to scale the permanent dipole moment of a water molecule as a function of the ion–water distance. From a methodological point of view this approach benefits from the strong radial orientation of the water dipole vectors in the first hydration shell around a charge of +3. This new potential function model involves three-body forces for the water–ion–water interaction within the first hydration shell. It allows a reasonable fit to ab-initio data, and computational costs for the simulation are only slightly increased compared to a nonpolarizable model. In the simulations the reinforcement of the ion–water interaction outweighs the increase of the water–water

repulsion within the first hydration shell and results in better defined first hydration shells and in a more balanced overall reproduction of experimentally known structural and kinetic properties. All three simulations using the polarizable model lead to a clear plateau region in the running coordination number $CN_{ion-oxygen}(r)$—corresponding to a minimum close to zero in the pair distribution function $g_{ion-oxygen}(r)$—and therefore fulfill the experimentally determined condition that structural hydration numbers CN should have integer values. These come out either as 9.0 and 8.0 or as an equilibrium between 8- and 9-fold coordination, in perfect agreement with coordination numbers from neutron diffraction studies.[4] The cation causes a high degree of structural order in its surroundings that extends well beyond the first hydration sphere. The dipole vectors of water molecules in the second sphere are still preferentially radially aligned, and the first and second hydration shells are firmly linked by two linear hydrogen bonds per water molecule in the first sphere. A preferential orientation of water molecules in the second coordination shell has been experimentally observed for the Ni^{2+} ion.[26] The simulated water exchange kinetics is equal (Nd^{3+}) or up to 50 times too fast (Yb^{3+}) compared to the experimental data. For a 1 order of magnitude difference in the exchange rate constant the error in terms of the free energy of activation $\Delta G^{\ddagger}$ can be estimated as $\pm RT \ln 10 = \pm 6$ kJ/mol, and is acceptable given the precision of the applied potential energy function and the experimental values between 22 and 30 kJ/mol for $\Delta G^{\ddagger}$ of the heavy lanthanide octa aqua ions (see, e.g., the compilation of $\Delta G^{\ddagger}$ values in ref 6c).[27] There remains the apparent contradiction that the simulations yield too negative hydration enthalpies, even though the applied potential function is partially based on ab-initio calculations at the Hartree—Fock level that give too low binding energies (cf. Figure 1 and the binding energy of one water molecule at the Hartree—Fock and at the MP2 level).

In their MD study of aqueous $LaCl_3$ solutions Meier et al.[7] reported a concentration dependent coordination number for the La^{3+}—aqua ion that increases from 10.2 at 2 *m* concentration to 12 at "infinite" dilution (1 La^{3+} ion and 200 water molecules). These numbers are, therefore, always higher than the values observed in our work for a concentration (1 La^{3+} ion and 300 water molecules, $c_{Ln^{3+}} = 0.19$ *m*) that is even lower than that of the most dilute solution studied in ref 7. In addition, coordination numbers from neutron diffraction studies on 0.3 and 1.0 *m* $Ln(ClO_4)_3$ solutions are identical within experimental error, both for the case of Dy^{3+} [4a] and for the case of Nd^{3+}.[4c] It was therefore concluded in ref 4c that the structure of the Ln^{3+} hydration sphere in aqueous perchlorate solutions is independent of concentration up to 1 *m*, and that $CN_{ion-oxygen}(r)$ obtained at 1 *m* are identical to those at infinite dilution.

The current understanding of the experimental data for the water exchange on the lanthanide aqua ions is based on the change of the relative stability of the ennea aqua and octa aqua ions across the series.[6b] It is in the first place assumed that a 9-coordinated species exchanges water via an intermediate or transition state of coordination number 8, whereas an 8-coordinated species exchanges via an ennea aqua ion. The second assumption is that toward the heavier and smaller lanthanide ions the stability of an ennea aqua ion decreases, whereas the stability of an octa aqua ion increases. The resulting small energy gap between 8- and 9-fold coordination for the lanthanide aqua ions around Sm^{3+} yields small activation energies and hence high exchange rates. The experimental evidence for this model is the following. For Sm^{3+} a coordination number of 8.5_4 has been measured by neutron diffraction,[4b,4c] and from the relative width of the first peak in $g_{ion-oxygen}(r)$ along the series of Ln^{3+} ions, such a coordination number has been interpreted as an equilibrium between an 8-fold and a 9-fold coordinated species.[4c] Due to the unfavorable magnetic properties of the light lanthanide aqua ions NMR kinetic experiments have up to now only allowed a lower limit for the exchange rate on the Nd^{3+}—aqua ion to be determined.[6c] The existence of a maximum of the kinetic lability of the first hydration shell in the middle of the series around Sm^{3+} can therefore still not be unambigously confirmed from an experimental point of view (see k_{ex}^{298} in Table 1). However, additional information comes from complex formation reactions of the Ln^{3+}—aqua ions. The rate constants of the interchange of a water molecule from the first hydration sphere with a SO_4^{2-} ion from the second sphere are experimentally known across the whole series of lanthanides.[25] These values are closely correlated with the known water exchange rates k_{298} for the heavy lanthanides between Gd^{3+} and Yb^{3+} [6c] and show indeed a maximum in the middle of the series.

On the whole, our simulations fit into the aforementioned model. Hydration shells with an integer number of water molecules (i.e., 8 or 9) are of minimum kinetic lability. A CN of 8.5 (simulation Sm) corresponds to an equilibrium of equal amounts of a 9-coordinated and an 8-coordinated Ln^{3+} ion and supports the fact that a Ln^{3+}—aqua ion is able to assume two equally stable states of different coordination numbers. In this case the very frequent shuttling of a ninth water molecule between the first hydration shell and the bulk results in a significant lowering of the residence time of water molecules in the first hydration shell, compared to Ln^{3+}—aqua ions with integer coordination numbers. It would be challenging to calculate separately the energy gap between the octa and the ennea species on the one hand and the activation barrier for a dissociatively and a associatively activated transition between both species on the other and to follow these quantities along the series in order to quantify both their thermodynamic and kinetic properties.

Acknowledgment. This work was supported by the Swiss National Science Foundation (Grant No. 20-39483.93) and the Swiss OFES as part of the European COST D3 action.

JA943674G

(25) Fay, D. P.; Litchinsky, D.; Purdie, N. *J. Phys. Chem.* **1969**, *73*, 544.

(26) Powell, D. H.; Neilson, G. W.; Enderby, J. E. *J. Phys.: Condens. Matter* **1989**, *1*, 8721—8733.

(27) Note that—contrary to the experimental data—the water exchange rates in the simulations are slightly higher for the octa aqua ion than for the ennea aqua ion. This deficiency is probably linked to the limited flexibility of the applied potential function model. Even after optimization of the parameter set used for the ion—water Lennard-Jones interaction a coordination number of 8 remained slightly less well defined than 9 (Figure 3). Correspondingly, in the simulation Yb, in 5% of all configurations (Figure 5), a water molecule is present between the first and second hydration shells and leads to higher exchange rates than for the ennea aqua ion. Further, it should be added that cation—water potential energy surfaces from the ab-initio calculations show less curvature than the empirical surfaces (see Figure 1) and would probably further increase water exchange rates. On the other hand, if a value of $f = 0.35$ were used for Yb^{3+} as discussed in section 2.4, it would likely decrease the water exchange rate and lead to a better agreement with experimental data.